Free-Energy Dissipations via Surface Intermediates Evaluated by the Frequency Response Method in a Catalystic Hydrogenation of Propene over Rhodium

Yusuke Yasuda* and Yasuhiro Kuno

Faculty of Science, Toyama University, Toyama 930, Japan

Received: December 2, 1998; In Final Form: March 3, 1999

Free-energy dissipations via various surface intermediates on Rh-metals in the catalytic hydrogenation of propene at 314 K are evaluated from the values of a novel rate constant l (Yasuda and Kuno, 1998) determined empirically by the frequency response (FR) method, where a cell reactor composed of a proton-conducting membrane was adopted; hydrogen and propene were separated by the membrane in order to investigate separately various rate processes due to either hydrogen or propene. The dissipations concluded are (i) $-0.27\mu_{HZ}\bar{R}$ and $-0.45\mu_{HZ}\bar{R}$ via the surface intermediates H_2(a) and H(a), respectively, and (ii) $+1.62\mu_{EZ}\bar{R}$ and $-1.31\mu_{EZ}\bar{R}$ via the intermediates C_3H_6(a) and C_3H_7(a), respectively; μ_{HZ} denotes the difference between chemical potentials of the reactant and product given by $\mu(H_2(g))-\mu(C_3H_8(g))$ and μ_{EZ} is the difference given by $\mu(C_3H_6(g))-\mu(C_3H_8(g))$; $\bar{R}$ is the appearance rate of propane. Because free energy of a system must dissipate in the course of any reaction according to the second law of thermodynamics, the stage accompanied by $+1.62\mu_{EZ}\bar{R}$ (> 0) cannot occur spontaneously and therefore that stage may be regarded as the "real" rate-determining step. Because free-energy dissipation via an intermediate is expected to play a fundamental role in a catalytic reaction, the present FR method could open new aspects of heterogeneous catalysis in a kinetic study.

1. Introduction

1.1. Kinetic Model Based on Free-Energy Dissipations. A traditional rate equation for a chemical reaction is usually based on material balance with respect to a component on the basis of mass conservation law. For instance, in the reaction mechanism shown in Figure 1, the material balance concerned with the intermediates A and B leads to

$$dA/dt = S_I - S_{II} \quad (1)$$

and

$$dB/dt = S_{II} - R \quad (2)$$

where A and B denote the amounts of the intermediates; S_I, S_{II}, and R denote the net reaction rates at the first, second, and third stage, respectively.

On the other hand, according to the second law of thermodynamics, the Gibbs free energy of a reactive system keeps decreasing in the course of any reaction under conditions of constant pressure and temperature. Nevertheless, free-energy dissipation of the system has scarcely been considered in deriving a rate equation probably because of the lack of experimental techniques. It should be emphasized, however, that the free-energy dissipation is expected to play a fundamental role in chemical kinetics just as an energy conservation law plays an essential role in mechanical kinetics.

A frequency response (FR) method has successfully been applied to determine various rate coefficients of gas/surface dynamic phenomena.[1] In the first application of the method to a catalytic reaction, an unordinary rate equation was required to interpret FR data.[2] To confirm the unexpected result, more rigorous experiments were carried out by a sophisticated reactor composed of a proton-conducting membrane.[3] Although complex rate constants, $(k + i\omega l)$, have been found to be indispensable to reproduce the FR data, a working hypothesis was needed to justify the novel rate constant l,[3] where k denotes the ordinary rate coefficient and ω is the angular frequency when the FR measurement was carried out.

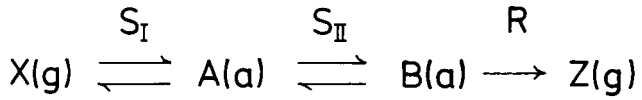

Figure 1. Three-stage model for a catalytic reaction. X(g) denotes the reactant in gas phase; A(a) and B(a) are the intermediates on catalysts; Z(g) is the product in gas phase; S_I, S_{II}, and R are the net reaction rates at the first, second, and third stage, respectively.

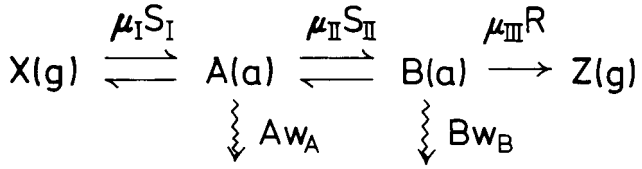

Figure 2. Flow of free energy in the three-stage model in Figure 1. μ_I, μ_{II}, and μ_{III} denote the free energy drops at the first, second, and third stage, respectively; w_A and w_B are the molar free-energy dissipations via the intermediates A and B, respectively.

Recently, a novel kinetic model for a catalytic reaction based on the free-energy dissipations illustrated in Figure 2 has been proposed to explain the complex rate constants without the hypothesis.[4] "Free-energy balances" can be expressed in this model by

$$Aw_A = \mu_I S_I - \mu_{II} S_{II} \quad (3)$$

* To whom correspondence should be addressed. E-mail: yasuda@sci.toyama-u.ac.jp. Fax: +81 764 45 6549.

10.1021/jp984575i CCC: $18.00
Published on Web 04/24/1999

and

$$Bw_B = \mu_{II}S_{II} - \mu_{III}R \quad (4)$$

where w_A and w_B are the molar free-energy dissipations via A and B, respectively; μ_I, μ_{II}, and μ_{III} are the free energy drops at each stage given by

$$\mu_I \equiv \mu_X - \mu_A, \qquad \mu_{II} \equiv \mu_A - \mu_B, \qquad \mu_{III} \equiv \mu_B - \mu_Z \quad (5)$$

Here μ_X , μ_A , μ_B , and μ_Z denote the chemical potential of every molecular species.

The aim of this article is to propose a theoretical procedure to evaluate w_A and w_B from the novel rate constant l on the basis of actual FR data obtained in a catalytic hydrogenation of propene.

1.2. Novel Rate Constant (*l*). A catalytic hydrogenation of light olefins has been the subject of intensive investigations[5,6] as one of the basic catalytic reactions and a three-stage model of

$$X(g) \underset{S_{-I}}{\overset{S_{+I}}{\rightleftharpoons}} A_X(a) \underset{S_{-II}}{\overset{S_{+II}}{\rightleftharpoons}} B_X(a) \xrightarrow{R} Z(g) \quad (6)$$

has widely been accepted,[7−9] where S_{+I} and S_{-I}, for example, denote the direct and reverse reaction rates at the first-stage; X(g) denotes the reactant of hydrogen (or olefins) in gas phase; $A_X(a)$ and $B_X(a)$ are the surface intermediates arising from X; and Z(g) is the product in gas phase (for instance, ethane) of which the reverse reaction can be neglected.

In the FR method, a reaction at a steady state is perturbed sinusoidally. The variation caused by the perturbation can be represented by $S_{+I}(t) = \bar{S}_{+I} + \Delta S_{+I}(t)$, $S_{-I}(t) = \bar{S}_{-I} + \Delta S_{-I}(t)$, $\bar{A}_X(t) = A_X + \Delta A_X(t)$, etc.; the bar on the letter indicates the value at the steady state. Because the perturbation is usually small enough, any rate equation can be linearized so that we may derive linear relations between various variations; for example,

$$\Delta S_{+I}(t) = K_{PX}\Delta P_X(t), \qquad \Delta S_{-I}(t) = k_{-AX}\Delta A_X(t), \qquad \text{etc.} \quad (7)$$

It has been shown further that the variations concerned with $\Delta S_{+II}(t)$ and $\Delta R(t)$ can be expressed as[4]

$$\Delta S_{+II}(t) = (k_{AX} + i\omega l_{AX})\Delta A_X(t) \qquad \text{and}$$
$$\Delta R(t) = (k_{BX} + i\omega l_{BX})\Delta B_X(t) \quad (8)$$

Here K and k are defined as the coefficients of a Taylor-series expansion at the steady state of the reaction (which will be indicated by subscript s):

$$K_{PX} \equiv (\partial S_{+I}/\partial P_X)_s, \qquad k_{-AX} \equiv (\partial S_{-I}/\partial A_X)_s,$$
$$k_{AX} \equiv (\partial S_{+II}/\partial A_X)_s,$$
$$k_{-BX} \equiv (\partial S_{-II}/\partial B_X)_s, \qquad k_{BX} \equiv (\partial R/\partial B_X)_s \quad (9)$$

On the other hand, the novel rate constant l_{AX} and l_{BX} are expressed by

$$l_{AX} \equiv (\partial S_{+II}/\partial \dot{A}_X)_s \qquad \text{and} \qquad l_{BX} \equiv (\partial R/\partial \dot{B}_X)_s \quad (10)$$

The dot on the letter means the time derivative, $\dot{A} \equiv dA/dt$ and $\dot{B} \equiv dB/dt$, and ω is the angular frequency where the FR measurements are carried out. It is worth noting that these l's disappear in a steady-state kinetic measurement because of $\omega = 0$ in this case.

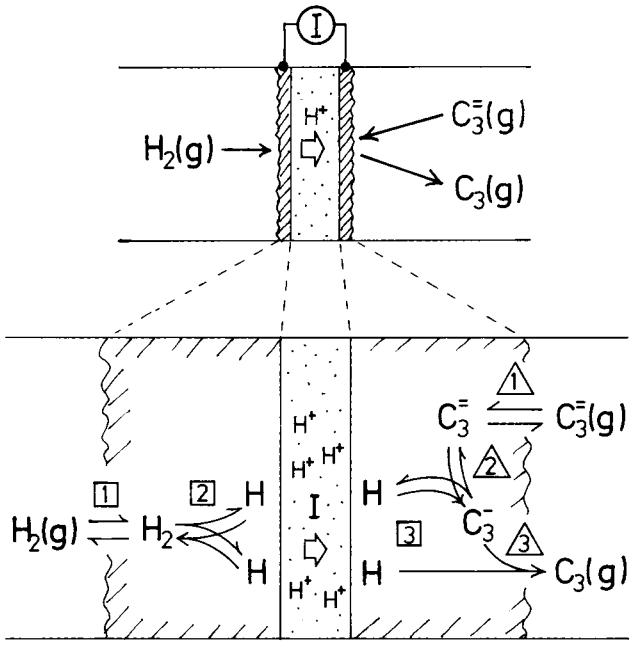

Figure 3. Cell reactor composed of a proton-conducting membrane, on both sides of which Rh is chemically deposited. Hydrogen and propene(C_3^{2-}) are separated by the membrane. Reaction mechanisms (based on the three-stage model in Figure 1) for the reactions on both sides of the membrane are extensionally illustrated in the lower part.

Consequently, the reaction mechanism in eq 6 can be characterized by seven parameters:[4]

$$X(g) \underset{k_{-AX}}{\overset{K_{PX}}{\rightleftharpoons}} A_X(a) \underset{k_{-BX}}{\overset{k_{AX} + i\omega l_{AX}}{\rightleftharpoons}} B_X(a) \xrightarrow{k_{BX} + i\omega l_{BX}} Z(g) \quad (11)$$

Evidently, eq 11 agrees with the traditional one if $l_{AX} = 0$ and $l_{BX} = 0$ are satisfied.

2. Experimental Section

2.1. FR Method. The apparatus composed of a proton-conducting membrane and the procedure have been described elsewhere.[3] The cell reactor is outlined in Figure 3. Here the short notation, $H_2(P_H)/Rh//Rh/C_3^{2-}(P_E)$, is introduced which means that hydrogen and propene(C_3^{2-}) was separated by the membrane on both sides of which Rh was chemically deposited. The pressure of either hydrogen, P_H, or propene, P_E, was perturbed at a steady state by changing the volume of gas space sinusoidally, of which variation was expressed well by (using complex notation)

$$P_X(t) = \bar{P}_X + \Delta P_X(t);$$
$$\Delta P_X(t) = \Delta P_X \exp(i\omega t) \text{ (X = H or E)} \quad (12)$$

The bar indicates the value at the steady state before (and/or after) the FR measurements.

The FR of the system was observed by current I due to the flow of H^+, which may be expressed in general by

$$I_X(t) = \bar{I}_X + \Delta I_X(t); \qquad \Delta I_X(t) = \Delta I_X \exp\{i(\omega t + \psi_X)\} \quad (13)$$

where ψ_X denotes the phase difference between $\Delta I_X(t)$ and $\Delta P_X(t)$.

The reaction mechanisms on both sides of the membrane (corresponding to the three-stage model in eq 6) are extension-

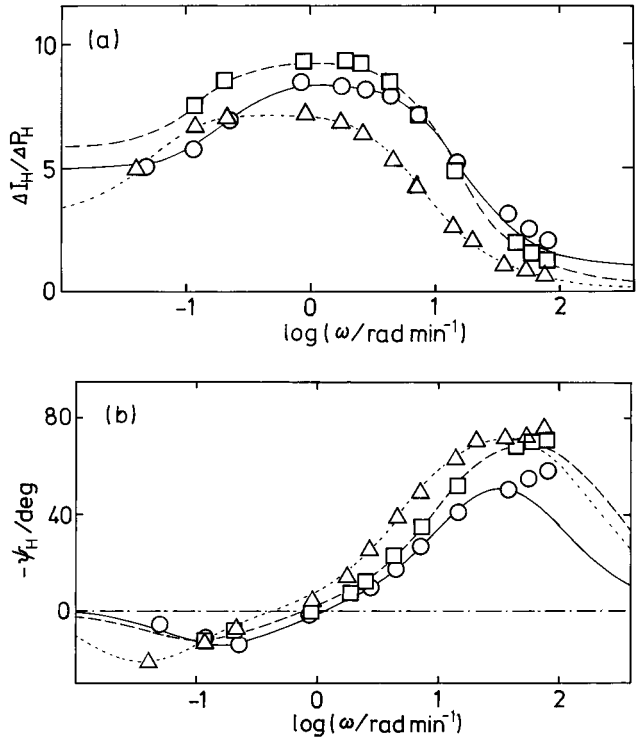

Figure 4. FR data of $H_2(\bar{P}_H)$/Rh//Rh/C_3^{2-}(20 Torr). (a) $\Delta I_H/\Delta P_H$(μA/Torr) versus ω. (b) ψ_H versus ω. $\bar{P}_H$/Torr = 10(△), 20(□), or 40(○), while $\bar{P}_E$/Torr = 20 in each run. The three kinds of curves represent the calculated results of $J_H^*(\omega)$ evaluated by each set of the seven parameters in Table 1.

ally illustrated in the lower part of Figure 3. The variation in the current, $\Delta I_X(t)$, induced by $\Delta P_X(t)$ can be described by[4]

$$\Delta I_X(t) = J_X^*(\omega)\Delta P_X(t) \tag{14}$$

where

$$J_X^*(\omega) \equiv K_{PX}k_{AX}^*(2k_{BX}^* + i\omega)/\Gamma_X \tag{15}$$

Here the following short notation has been introduced:

$$k_{AX}^* \equiv k_{AX} + i\omega l_{AX}, \qquad k_{BX}^* \equiv k_{BX} + i\omega l_{BX},$$
$$\Gamma_X \equiv (k_{-AX} + k_{AX}^* + i\omega) \times (k_{-BX} + k_{BX}^* + i\omega) - k_{AX}^* k_{-BX} \tag{16}$$

Because the ratio $\Delta I_X(t)/\Delta P_X(t) = (\Delta I_X/\Delta P_X)\exp(i\psi_X)$ (X = H or E) can be determined empirically, the seven parameters involved in the characteristic function $J_X^*(\omega)$ in eq 15 can be determined by computer simulation to reproduce FR data as close as possible over the whole range of ω scanned. The subscript X will often be omitted for simplicity.

3. Results

Two series of the FR measurements were carried out in this work under different combinations of $\bar{P}_H$ and $\bar{P}_E$: (i) $\bar{P}_H$/Torr = 10, 20, and 40, while $\bar{P}_E$/Torr = 20 and (ii) $\bar{P}_H$/Torr = 20, while $\bar{P}_E$/Torr = 10, 20, and 40 (1 Torr = 133.32 Pa).

3.1. FR Data. The ratio of the amplitude, $\Delta I_H/\Delta P_H$, and the phase difference, ψ_H, which were observed in series (i) are plotted versus ω in Figures 4a and 4b, respectively. The two kinds of FR data are plotted together in Figure 5.

On the other hand, those results obtained in series (ii) are shown in Figures 6a and 6b, and they are combined in Figure 7.

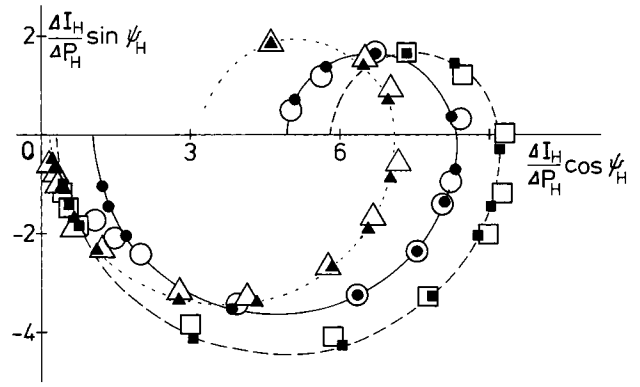

Figure 5. Polar plots of ($\Delta I_H/\Delta P_H$, ψ_H) shown in Figures 4a and 4b. The solid symbols (corresponding to the open symbols) represent the simulated results for the FR data evaluated by the seven parameters in Table 1. Notation is that of Figure 4.

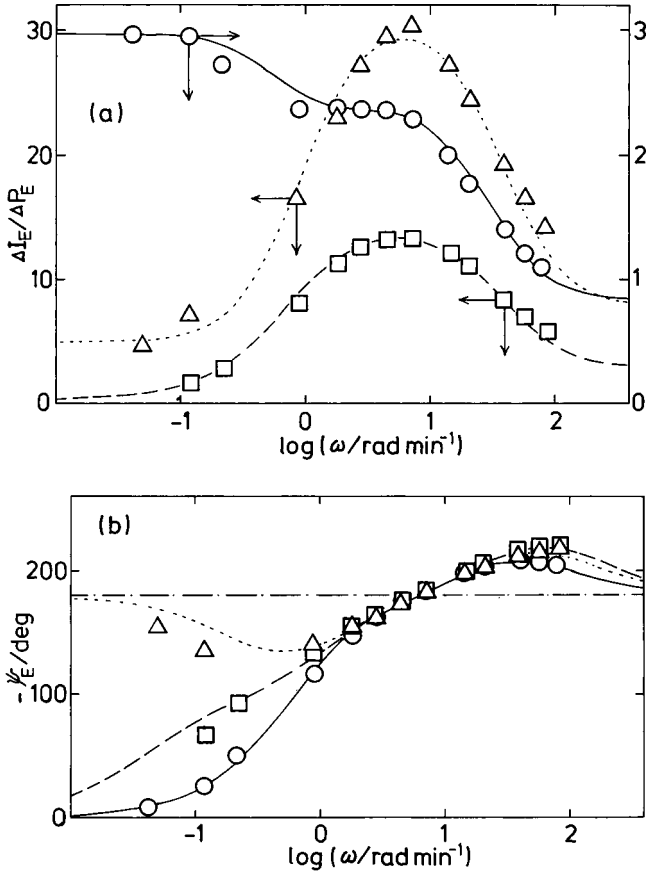

Figure 6. FR data of H_2(20Torr)/Rh//Rh/$C_3^{2-}(\bar{P}_E)$. (a) $\Delta I_E/\Delta P_E$(μA/Torr) versus ω. (b) ψ_E versus ω. $\bar{P}_E$/Torr = 10(△), 20(□), or 40(○), while $\bar{P}_H$/Torr = 20 in each run. Each curve represents the calculated results of $J_E^*(\omega)$ evaluated by the seven parameters in Table 2.

3.2. Data Analysis. Computer simulation by $J_H^*(\omega)$ (or $J_E^*(\omega)$) in eq 15 for actual FR data was carried out on a trial-and-error basis. The calculated results are compared with the experimental ones by the three kinds of curves in Figure 4 (or Figure 6) and also by the solid symbols in Figure 5 (or Figure 7). The seven parameters evaluated by the simulation in series (i) and (ii) are summarized in Tables 1 and 2, respectively; they are also plotted versus $\bar{P}_H$ or $\bar{P}_E$ in Figure 8. Another set of the seven parameters evaluated by a separate simulation repeated for the same FR data are compared by the solid symbols in Figure 8 in order to show the accuracy of each coefficient.

It seems of interest that both l_{AH} and l_{BH} are positive, while both l_{AE} and l_{BE} are negative as will be discussed below.

TABLE 1: Experimental Conditions and Rate Coefficients in J_H* Evaluated by Computer Simulation for the FR Data of $H_2(\bar{P}_H)$/Rh//Rh/C_3^{2-} (20 Torr) in Figure 5

$\bar{P}_H$ (Torr)	E_s[a] (mV)	I_s (mA)	K_{PH} (mA/Torr)	k_{-AH} (/min)	k_{AH} (/min)	k_{-BH} (/min)	k_{BH} (/min)	l_{AH}	l_{BH}	dev[b] (%)
10	−15.62	0.063	0.0381	4.68	0.764	0.070	0.026	0.0038	0.525	2.15
20	−16.33	0.134	0.0311	7.55	2.10	0.160	0.095	0.0075	0.609	1.99
40	−17.72	0.275	0.0172	7.80	4.04	0.363	0.175	0.0477	0.819	2.94

[a] The negative value of E_s means that the current I_s was hindered by the supplied voltage. [b] dev $\equiv (1/N)\sum_N[\{(\Delta I_H/\Delta P_H)_N - J_H^*(\omega_N)_{calc}\}^2]^{1/2}/(\Delta I_H/\Delta P_H)_{max}$ (N: no. of data).

TABLE 2: Experimental Conditions and Rate Coefficients in J_E* Evaluated by Computer Simulation for FR Data of H_2 (20 Torr)/Rh//Rh/$C_3^{2-}(\bar{P}_E)$ in Figure 7

$\bar{P}_E$ (Torr)	E_s[a] (mV)	I_s (mA)	K_{PE} (mA/Torr)	k_{-AE} (/min)	k_{AE} (/min)	k_{-BE} (/min)	k_{BE} (/min)	l_{AE}	l_{BE}	dev[b] (%)
10	−16.12	0.113	0.0984	1.196	−0.131	4.67	1.359	−0.624	−0.488	3.97
20	−16.15	0.116	0.0498	0.916	0.021	4.97	1.303	−0.602	−0.490	3.10
40	−17.53	0.256	0.0239	0.456	0.347	4.69	0.448	−0.570	−0.493	2.83

[a] The negative value of E_s means that the current I_s was hindered by the supplied voltage. [b] dev $\equiv (1/N)\sum_N[\{(\Delta I_E/\Delta P_E)_N - J_E^*(\omega_N)_{calc}\}^2]^{1/2}/(\Delta I_E/\Delta P_E)_{max}$ (N: no. of data).

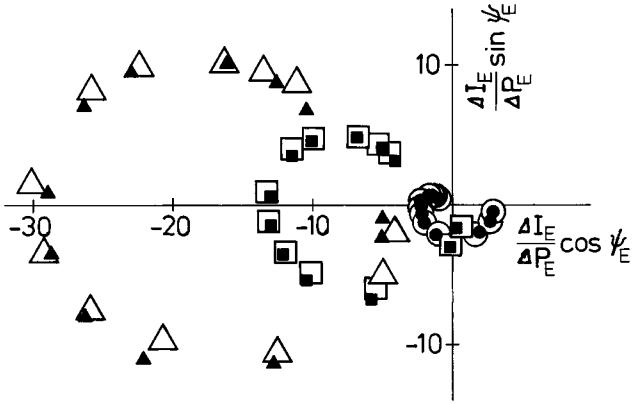

Figure 7. Polar plots of ($\Delta I_E/\Delta P_E$, ψ_E) shown in Figures 6a and 6b. The solid symbols (corresponding to the open symbols) represent the simulated results for the FR data evaluated by the seven parameters in Table 2. Notation is that of Figure 6.

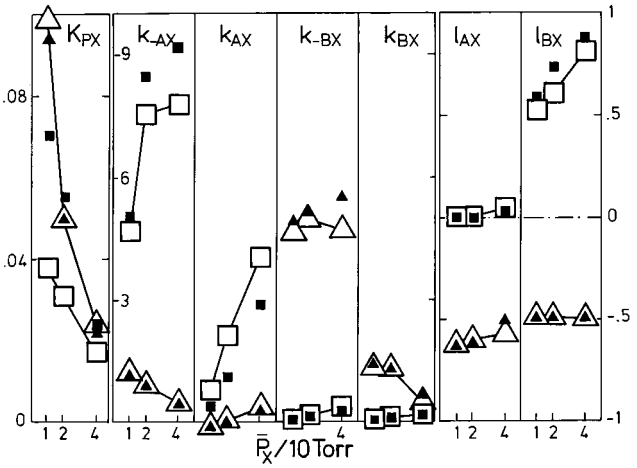

Figure 8. Rate coefficients obtained in the computer simulation, K_{PX}/(*m*A/Torr), k/min^{-1}, and l summarized in Tables 1 and 2 are plotted as functions of $\bar{P}_H$(□) and $\bar{P}_E$(△). The solid symbols represent the results obtained in another separate simulation for the same FR data.

4. Theoretical Section

4.1. Expressions for μ_I, μ_{II}, and μ_{III}. At a steady state of the reaction, eqs 1 and 2 lead to

$$\bar{S}_I = \bar{S}_{II} = \bar{R} \tag{17}$$

Substituting eq 17 into eq 3 and 4, we have

$$\overline{Aw}_A = (\mu_I - \mu_{II})\bar{R} \tag{18}$$

and

$$\overline{Bw}_B = (\mu_{II} - \mu_{III})\bar{R} \tag{19}$$

When the system at the steady state is perturbed *in a way*, every variable in Figures 1 and 2 would also be perturbed. The variations of w_A and w_B, Δw_A and Δw_B, can be described by[4]

$$\Delta w_A = \{\mu_I + l_A(\mu_I - \mu_{II})\}\Delta\dot{A}/\bar{A} \tag{20}$$

and

$$\Delta w_B = \{\mu_{II} + l_B(\mu_{II} - \mu_{III})\}\Delta\dot{B}/\bar{B} \tag{21}$$

On the other hand, it should be emphasized that the free-energy dissipations are expressed by Aw_A and Bw_B in eq 3 and 4, which implies that w_A and w_B are independent of A and B and therefore could not be affected by $\Delta P_X(t)$ so that we have

$$\Delta w_A = \Delta w_B = 0 \tag{22}$$

Substituting eq 22 into eq 20 and 21, we get

$$\mu_I + l_A(\mu_I - \mu_{II}) = 0 \tag{23}$$

and

$$\mu_{II} + l_B(\mu_{II} - \mu_{III}) = 0 \tag{24}$$

Further, the definition for μ in eq 5 leads to

$$\mu_I + \mu_{II} + \mu_{III} = \mu_X - \mu_Z \ (\equiv \mu_{XZ}) \tag{25}$$

Solving the simultaneous equations of eq 23−25, we get the final results of

$$\mu_I = (l_A l_B/L)\,\mu_{XZ} \tag{26}$$

$$\mu_{II} = \{(1 + l_A)l_B/L\}\mu_{XZ} \tag{27}$$

$$\mu_{III} = \{(1 + l_A)(l + l_B)/L\}\mu_{XZ} \tag{28}$$

where the short notation has been used:

$$L \equiv 1 + l_A + 2l_B + 3l_A l_B \tag{29}$$

TABLE 3: Free-Energy Drops at the First, Second, and Third Stage Concerned with Hydrogen, μ_{IH}, μ_{IIH}, and μ_{IIIH}, and Free-Energy Dissipations via A_H- and B_H-species, $\bar{A}_H\bar{w}_{AH}$ and $\bar{B}_H\bar{w}_{BH}$, Respectively

$\bar{P}_H$ (Torr)	μ_{IH} (μ_{HZ})	μ_{IIH} (μ_{HZ})	μ_{IIIH} (μ_{HZ})	$\bar{A}_H\bar{w}_{AH}$ (μ_{HZ} R)	$\bar{B}_H\bar{w}_{BH}$ (μ_{HZ} R)	$(\bar{A}_H\bar{w}_{AH} + \bar{B}_H\bar{w}_{BH})$ (μ_{HZ} R)
10	0.001	0.256	0.743	−0.255	−0.487	−0.742
20	0.002	0.274	0.724	−0.272	−0.450	−0.722
40	0.013	0.306	0.681	−0.293	−0.374	−0.667

TABLE 4: Free-Energy Drops at the First, Second, and Third Stage Concerned with Propene, μ_{IE}, μ_{IIE}, and μ_{IIIE}, and Free-Energy Dissipations via A_E- and B_E-species, $\bar{A}_E\bar{w}_{AE}$ and $\bar{B}_E\bar{w}_{BE}$, Respectively

$\bar{P}_E$ (Torr)	μ_{IE} (μ_{EZ})	μ_{IIE} (μ_{EZ})	μ_{IIIE} (μ_{EZ})	$\bar{A}_E\bar{w}_{AE}$ (μ_{EZ} R)	$\bar{B}_E\bar{w}_{BE}$ (μ_{EZ} R)	$(\bar{A}_E\bar{w}_{AE} + \bar{B}_E\bar{w}_{BE})$ (μ_{EZ} R)
10	0.970	−0.584	0.614	1.554	−1.198	0.356
20	0.974	−0.643	0.669	1.617	−1.312	0.305
40	0.980	−0.739	0.759	1.719	−1.499	0.221

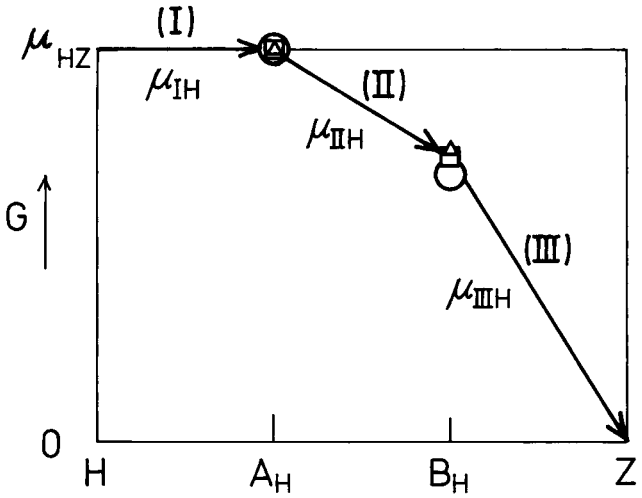

Figure 9. Free-energy drops at the first, second, and third stage concerned with hydrogen, μ_{IH}, μ_{IIH}, and μ_{IIIH}, given in Table 3. The symbols △, □, and ○ correspond to those in Figure 4.

4.2. Expressions for Free-Energy Dissipations. Substituting eq 26−28 into eq 18 and 19, we can easily find the expressions for $\overline{Aw}_A$ and $\overline{Bw}_B$:

$$\overline{Aw}_A = -(l_B/L)\mu_{XZ}\bar{R} \tag{30}$$

and

$$\overline{Bw}_B = -\{(1 + l_A)/L\}\mu_{XZ}\bar{R} \tag{31}$$

The total of the dissipations is given by

$$\overline{Aw}_A + \overline{Bw}_B = -\{(1 + l_A + l_B)/L\}\mu_{XZ}\bar{R} \tag{32}$$

It should be emphasized that l_A and l_B play essential roles in eq 26−32.

5. Discussion

5.1. Free-Energy Drops, μ_I, μ_{II}, and μ_{III}. Substituting the values of l from Tables 1 and 2 into eq 26−28, we can determine the values of μ_{IX}, μ_{IIX}, and μ_{IIIX}. The results in series (i) and (ii) are summarized in Tables 3 and 4, respectively. They are illustrated versus reaction coordinate in Figures 9 and 10, respectively. It seems of interest that

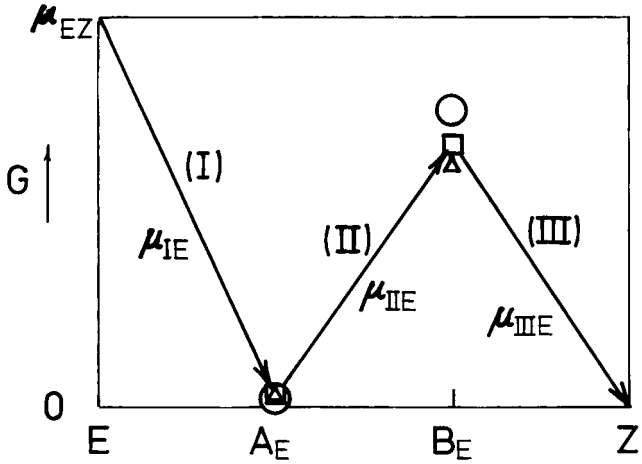

Figure 10. Free-energy drops at the first, second, and third stage concerned with propene, μ_{IE}, μ_{IIE}, and μ_{IIIE}, given in Table 4. The symbols △, □, and ○ correspond to those in Figure 6.

$$\mu_{IH} \doteqdot 0 \text{ and } \mu_{IIE} < 0 \tag{33}$$

The former means that the first-stage concerned with hydrogen is almost in equilibrium and may be omitted, which agrees with (unmodified) Horiuti−Polanyi mechanism.[7] The latter means that the process of $C_3H_6(a) \rightarrow C_3H_7(a)$ (see Figure 3) is against the reaction and needs some assistance.

5.2. Free-Energy Dissipations, $\bar{A}\bar{w}_A$ and $\bar{B}\bar{w}_B$. Substituting the values of l from Tables 1 and 2 into eq 30−32, we can obtain the values for $\bar{A}_X\bar{w}_{AX}$, $\bar{B}_X\bar{w}_{BX}$, and $\bar{A}_X\bar{w}_{AX} + \bar{B}_X\bar{w}_{BX}$. The results in series (i) and (ii) are summarized in Tables 3 and 4, respectively.

The Gibbs free-energy change under constant temperature, ΔG, may be expressed by

$$\Delta G = \Delta H - T\Delta S \tag{34}$$

Therefore, the free energy dissipation $\overline{Aw}_A$, for example, may be divided into two terms:

$$\overline{Aw}_A = (\dot{H}_A)_s + T_A(-\dot{S}_A)_s \tag{35}$$

where H_A and S_A denote the enthalpy and entropy of A-species, respectively. Because the amount of A-species is constant during the dissipation, $(H_A)_s$ may be regarded as almost constant (then $(\dot{H}_A)_s \doteqdot 0$) so that we have

$$-\overline{Aw}_A = T_A(\dot{S}_A)_s \tag{36}$$

Consequently, the second stage concerned with hydrogen, II_H, may be divided into two stages, II_H' and II_H'', which are illustrated in Figure 11; the dissipation $\bar{A}_H\bar{w}_{AH}$ (<0, see Table 3) occurs in II_H' where S_{AH} is increasing because of eq 36; because the process accompanied by $\dot{S}_{AH} > 0$ can occur spontaneously, A_H may transform spontaneously to A_H^0. The dissipation process can be represented by the vertical line in Figure 11, because differences in the enthalpies of A_H- and A_H^0-species may be neglected. In a similar way, stage III_H can be divided into III_H' and III_H''. It should be emphasized that in the other stages of I, II″, and III″, molecular species transform from X to A, from A to B, and from B to Z, respectively.

According to similar treatments for the results obtained in series (ii), we have the results shown in Figure 12. Since the results of $\bar{A}_E\bar{w}_{AE}$ in Table 4 are positive, the entropy of A_E-species decreases during the dissipation, which is indicated by

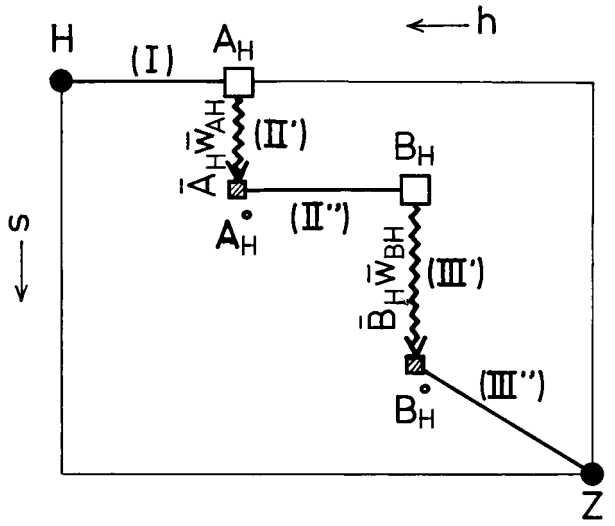

Figure 11. Free-energy dissipations of $\bar{A}_H\bar{w}_{AH}$ and $\bar{B}_H\bar{w}_{BH}$; *s* and *h* denote the molar entropy and molar enthalpy, respectively. Both entropies of A_H- and B_H-species increase but their enthalpies are kept almost constant during the dissipations. Therefore, the dissipations can be represented by the wavy vertical lines, II′ and III′. Transformation of molecular species accompanying enthalpy change from H_2(g) to A_H(a) occurs in the stage of I; that from A_H(a) to B_H(a) occurs in II″; that from B_H(a) to C_3(g), in III″.

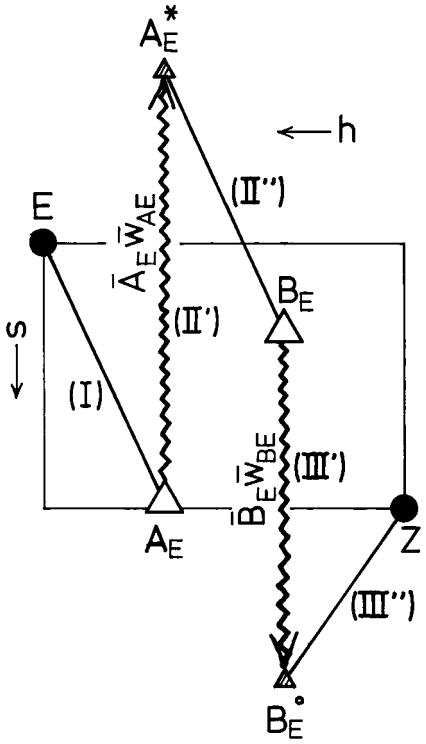

Figure 12. Free-energy dissipations of $\bar{A}_E\bar{w}_{AE}$ and $\bar{B}_E\bar{w}_{BE}$. During the dissipations, entropy of A_E-species decreases while that of B_E-species increases; the dissipations can be represented by the wavy vertical lines, II′ and III′, because enthalpies of both intermediates are kept almost constant during the dissipations. Transformation of molecular species accompanying enthalpy change from C_3^{2-}(g) to A_E(a) occurs in the stage of I; that from A_E(a) to B_E(a) occurs in II″; that from B_E(a) to C_3(g), in III″.

A_E* instead of A_H^0 because the transfer accompanied by decreasing entropy cannot occur spontaneously.

5.3. Estimation $\bar{w}_{AH}$ and $\bar{w}_{BH}$. If every elementary rate in eq 6 is proportional to the pressure or the amount of intermediate, every rate coefficient in eq 9 becomes constant. However, the results in Figure 8 depended considerably on each pressure; for example, a steep decrease in K_{PH} (or K_{PE}) with increasing $\bar{P}_H$ (or $\bar{P}_E$) means that $\bar{S}_{+IH}$ (or $\bar{S}_{+IE}$) saturates with the increasing pressure.

Rough estimation for the values of $\bar{w}_{AH}$ and $\bar{w}_{BH}$ can be carried out as follows: The mean lifetimes of A- and B-species, τ_A and τ_B, can be evaluated from the values of $(k_{-A} + k_A)^{-1}$ and $(k_{-B} + k_B)^{-1}$, respectively, provided that each elementary rate is roughly proportional to $\bar{A}$ or $\bar{B}$ and therefore these coefficients may be regarded as constants. It is assumed further that the amounts of A- and B-species are proportional to τ_A and τ_B, respectively. Then we may have

$$(\bar{A}_H\bar{w}_{AH}/\bar{B}_H\bar{w}_{BH}) = (\tau_{AH}\bar{w}_{AH}/\tau_{BH}\bar{w}_{BH}) = \{(k_{-BH} + k_{BH})/(k_{-AH} + k_{AH})\}(\bar{w}_{AH}/\bar{w}_{BH}) \quad (37)$$

which is rewritten as

$$(\bar{w}_{AH}/\bar{w}_{BH}) = \{(k_{-AH} + k_{AH})/(k_{-BH} + k_{BH})\}(\bar{A}_H\bar{w}_{AH}/\bar{B}_H\bar{w}_{BH}) \quad (38)$$

Substituting the values of *k* in Table 1 and those of $\bar{A}_H\bar{w}_{AH}$ and $\bar{B}_H\bar{w}_{BH}$ in Table 3 into eq 38, we have

$$\bar{w}_{AH} \doteqdot 20\bar{w}_{BH} \quad (39)$$

It is concluded therefore that

$$|\bar{w}_{AH}| \gg |\bar{w}_{BH}| \quad (40)$$

5.4. New Aspects of Catalysis. In a traditional kinetic study, elementary rates such as *S* and *R* in eq 6[7–9] or turnover (overall) rates[10] have been investigated rather than *K* and *k* in eq 11 under some uncertain assumptions. However, it should be emphasized that no assumptions have been required in the present method except the three-stage model. It is worth noting that as many as seven parameters were able to be determined by scanning a wide range of ω (analogous to a spectroscopic method). The fact that *k* and *l* in eq 11 are independent of the amount of A and B as well as catalysts is very important because they can be compared directly with those obtained by other catalysts and also by other investigators.

Various new aspects of dynamic phenomena on catalysts have been found from surface science studies. For example, concentration waves of adsorbed species propagating from active zones and pattern formation of adsorbate concentrations on surfaces during heterogeneously catalyzed reactions have been observed.[11] It has also been demonstrated by Iwasawa that weakly adsorbed molecules can activate the reaction of strongly adsorbed intermediates, ultimately controlling the reaction path;[12] the kinetic phenomena are named "surface catalytic reactions assisted by gas-phase molecules".[13] However, it seems difficult to describe quantitatively these kinetic behaviors by traditional rate equations.[14]

The increasing entropies during the free energy dissipations in eq 40 (see Figure 11) suggest surface migration of the intermediates. Evidently, it seems of interest to combine the FR method with surface science techniques.

Extension of the present work based on the three-stage model in eq 6 to a two- or four-stage model would be easy, because only rate coefficient concerned with the direct reaction of an intermediate becomes complex.

5.5. Comparison with the Theory of Rate Processes. The theory of rate processes[15] has been accepted for a basic theory, where the chemical potential drops except for the final stage are assumed to be negligibly small and therefore eq 5 becomes in this case

$$\mu_{\mathrm{I}} = 0, \qquad \mu_{\mathrm{II}} = 0, \qquad \mu_{\mathrm{III}} = \mu_{\mathrm{XZ}} \tag{41}$$

Substituting eq 41 into eq 26−28, we have

$$l_{\mathrm{A}} = 0 \text{ and } l_{\mathrm{B}} = 0 \tag{42}$$

It seems of interest that when eq 42 is accepted, eq 11 agrees with the traditional one.

It is concluded therefore that the present theoretical results in eq 26−28 cover the theory of rate processes.

6. Conclusions

Free-energy dissipations via various surface intermediates have first been investigated quantitatively by the FR method. Because the dissipations are expected to play fundamental roles in chemical kinetics, the present method would open new aspects of not only heterogeneous catalysis but also various rate processes.

References and Notes

(1) Yasuda, Y. *Heterogen. Chem. Rev.* **1994**, *1*, 103.
(2) Yasuda, Y. *J. Phys. Chem.* **1989**, *93*, 7185.
(3) Yasuda, Y.; Iwai, K.; Takakura, K. *J. Phys. Chem.* **1995**, *99*, 17852.
(4) Yasuda, Y.; Kuno, Y. *J. Phys. Chem.* **1998**, *102*, 4878.
(5) Bond, G. C. *Catalysis by Metals*; Academic Press: London, 1962.
(6) Horiuti, J.; Miyahara, K. *Hydrogenation of ethylene on Metallic Catalysts*; NBS−NSRDS No.13; Government Printing Office: Washington, DC, 1968.
(7) Horiuti, J.; Polanyi, M. *Trans. Faraday Soc.* **1934**, *30*, 1164.
(8) Sato, S.; Iyama, T.; Miyahara, K. *J. Catal.* **1981**, *69*, 77.
(9) Rekoske, J. E.; Cortright, R. D.; Goddard, S. A.; Sharma, S. B.; Dumesic, J. A. *J. Phys. Chem.* **1992**, *96*, 1880.
(10) Ribeiro, F. H.; Schach von Wittenau, A. E.; Bartholomew, C. H.; Somorjai, G. A. *Catal. Rev.−Sci. Eng.* **1997**, *39*, 49.
(11) Ertl, G. *Adv. Catal*. **1990**, *37*, 213.
(12) Iwasawa, Y. *Acc. Chem. Res.* **1997**, *30*, 103.
(13) Yamaguchi, A.; Shido, T.; Asakura, K.; Iwasawa, Y. *Shokubai* **1998**, *40*, 360.
(14) Schueth, F.; Henry, B. E.; Schmidt, L. D. *Adv. Catal*. **1993**, *39*, 51.
(15) Glasstone, S.; Laidler, K. J.; Eyring, H. *The Theory of Rate Processes*; McGraw-Hill: New York, 1941.